Original Article

Received: 2021-04-17
Accepted: 2021-08-01

BCCR
2021, No 1, Vol 13 :63-71
www.bccrjournal.com

Effects of Gold Nanoparticles on Proton Therapy for Breast Cancer

Elham Ariyabod[1], Seyedeh Nasrin Hosseini Motlagh[2*],Saeed Mohammadi[3]

[1] Department of Physics, Payame Noor University (PNU), P.O.Box 4697-19395,Tehran, Iran.

[2] Department of Physics, Shiraz Branch, Islamic Azad University, Shiraz, Iran

[3] Department of Physics, Payame Noor University (PNU), P.O.Box 4697-19395,Tehran, Iran

Corresponding author: Seyedeh Nasrin Hosseini Motlagh
Email: hosseinimotlagh@hotmail.com

ABSTRACT

Background: Beam therapy, the most common and successful treatment used after surgery, plays an important role in treating cancer. In proton therapy, proton beam (PB) particles irradiate the tumor. To enhance the treatment of breast tumors, gold nanoparticles (GNPS) can be injected into the tumor simultaneously as irradiating the PB.

Methods: This paper aims to simulate the treatment of breast tumors by using PBs and injecting GNPs with different concentrations simultaneously. We introduced the breast phantom (BP), then we irradiated it with a proton pencil beam, which is also injected with GNPs simultaneously. We used the GEANT4/ GATE7 (G4/G7) code to show the enhancement of the absorbed dose in the tumor.

Results: The findings of our simulations show that the location of the Bragg peak within the tumor shifts to higher depths with increasing energy. Also, by injecting GNPs in different amounts of 10, 25, 50, and 75 mg/ml with simultaneous irradiation of the PB, the rate of absorbed dose increases up to 1.75% compared to the non-injected state. Our results also show that the optimal range of proton energy that creates the Bragg peaks within the tumor is between 28 to 35 MeV, which causes the spread out of the Bragg peak. It should be noted that the amount of absorbed dose is affected by quantities such as total stopping power, average Coulomb scattering angle, CSDA range, and straggling range.

Conclusion: This work offers new insights based on the use of GNPS in the treatment of breast cancer through proton therapy and indicates that adding GNPS is a promising strategy to increase the killing of cancer cells while irradiating fast PBs. In fact, the results of this study confirm the ability of GNPs to enhance treatment by increasing the absorbed dose in breast tumors using proton therapy.

Keywords: Breast, Cancer, Nanoparticles ,Proton Therapy, Range,

INTRODUCTION:

Nowadays, hadron therapy with heavy charged particles is a modern technique in radiotherapy, so that it has physical and radiobiological advantages and, in general, has beneficial clinical properties. Physically, due to the optimal dose distribution of heavy-charged particles, healthy tissues can be significantly protected from unwanted damage, reducing side effects and secondary cancers. In addition, from a radiobiological point of view, the Relative Biological Effectiveness (RBE) of these particles is higher than that of photons, thereby increasing the efficiency of killing cancer cells and increasing the probability of tumor control. Thus, this technique is considered the preferred and definitive method in terms of cancer treatment. From a DNA damage perspective, it can be argued that cancer treatment uses the proton hadron beam to damage the DNA of cancer cells without destroying healthy cells. However, in X-ray therapy, nearby non-cancerous cells are also destroyed.

In recent years, using high-Z nanoparticles (NPs) for tumor activation to increase absorbed dose inside it is presented. Different studies have been performed on the effects of NPs such as gold, silver, platinum, and gadolinium combined with ionizing radiation (1-3). If GNPs with high Z target tumor, they can increase specifically absorbed dose focusing on the tumor, thereby minimizing the radiation damages on the healthy tissues (4). Lin et al. used Monte Carlo simulations to differentiate between two types of interactions: nanoparticle interactions on photons and protons. They found that the former increased more significantly than the latter (5). Lin et al. presented a biological model in which protons require NPs with higher concentrations than photons to have the same effectiveness (6). Porcello et al. (7), and Jane et al. (8) Investigated the simulations of Gold (Au), Silver (Ag), and Platinum (Pt), and confirmed that these materials are compatible with each other to participate in treatment (9). Gao and Zheng studied Monte Carlo simulation. They simulated a water phantom on a GNP. They concluded that the production of secondary electrons is increased with the reduction of proton energy. Kewon et al. simulated a GNP in water (10). They proposed a radial dose distribution with respect to secondary electrons. They noticed that the effect of GNPs increased more than a few micrometers in length and a few nanometers in radius direction, respectively (11).

In this study, we used G4/G7 simulator while employing the technique of pencil beam to radiate proton toward the PB for the first time. The absorbed dose and other quantities were examined in two cases: when GNPs were not injected into the PB, and when GNPs were injected into it with selecting four concentrations of 10, 25, 50, and 75 ml/mg. Since the Coulomb scattering effect is one of the essential physical phenomena, we determine the mean scattering angle in both cases and compare the results.

In this work, we used the G4/G7 Monte Carlo (MC) code simulator for the first time with the proton irradiation method in the form of a pencil beam to the suggested PB, so that we could determine the absorbed dose and the related various quantities (mass stopping power, MCS, CSDA range and straggling proton range) in this phantom in two steps. In the first step, GNPs are not injected into the tumor, while in the second step, GNPs with 4 different concentrations of 10, 25, 50, and 75 mg/ml are injected into the tumor.

Material and methods

Since the purpose of this paper is the simulation of particle therapy of breast cancer tissue using PB radiation with injecting of GNPs, the following items are studied to achieve this goal.

Suggested BP containing tumor

We used a semi-cylindrical phantom with a radius of 10 cm and a height of 5 cm. The main tissue is a semi-cylinder with a radius of 9 cm and a height of 4 cm, while the thickness of fat and the skin tissue was defined as 3.0 cm and 2.0 cm, respectively. According to the breast position, the cylindrical tumor has a height of 2 cm and is placed inside the breast at a depth of 2 cm (Fig.1). Then, we transported the PB at the range of $3 \geq E$ (MeV) ≥ 250 toward the phantom, and examined the effect of the beam on the breast tumor. The source defined in this work is a circle with a radius of 25.0 mm, which has a

Gaussian energy distribution and is close to the phantom. We inserted the NPs into the tumor tissue using a mechanical injection method. Simultaneously, by injecting GNPs into cancerous tissue, a PB irradiates the phantom. Then we estimated the absorbed dose related to the two states i) without and ii) with injecting GNPs with PB radiation. Finally, we confirmed the effect of increasing the absorbed dose in the tumor by injection of NPs.

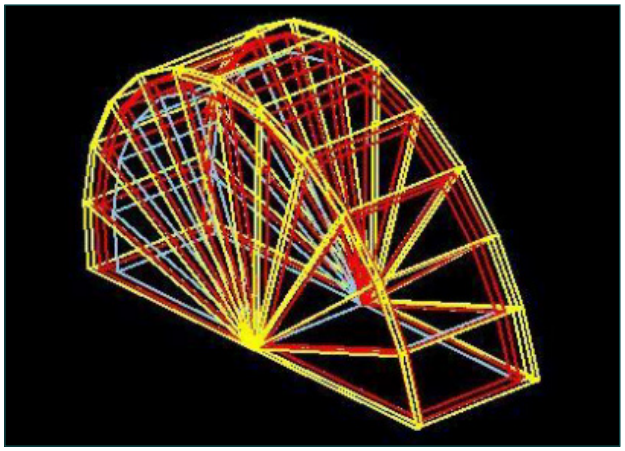

Figure.1. Simulated BP

Stopping power and absorbed dose

The energy loss of ions in a material is the main factor for determining ion distribution. An ion loses its energy (E) at the penetration depth (x), where x is the distance inside the target, measured from the target level. The lost energy in a material is called stopping power, represented by dE/dx. An energetic ion penetrating a material essentially loses its energy in two ways: a) nuclear energy loss (dE/dX_{nuc}) (b) electronic energy loss (dE/dX_{el}); they are independently examined. Thus, total power (S) is given by:

$$S = dE/dx = \frac{dE}{dx}_{nuc} + \frac{dE}{dx}_{el} \qquad (1)$$

The equation for the proton stopping power in a material is obtained by the quantum mechanical Bethe's equation [12]:

$$\frac{dE}{dx} = \frac{nz^2e^4}{4\pi\varepsilon_0^2 m_e v^2}\left[\left\{\ln\left(\frac{2m_e v^2}{I}\right)\right\} - \ln\left(1 - {}^{v^2}/_{c^2}\right) - {}^{v^2}/_{c^2}\right] \qquad (2)$$

where, Z= heavy-ion atomic number, e=elementary charge, n=number of electrons per unit volume of matter, c= the speed of light in vacuum, β= v/c, where v is the ion velocity and c is the light velocity in a vacuum, I= the mean excitation potential, ε0 = vacuum permittivity, and m_e= electron mass. Mass stopping power is obtained by: $\frac{1}{\rho}S = -\frac{1}{\rho}\frac{dE}{dx}$. In Fig.2, we compared the total mass stopping power of protons in PB using G4/G7 simulation for two cases: a) without b) injecting different concentrations of GNPs. The absorbed dose is the mean energy deposited in the matter by ionizing radiation per unit mass. The absorbed dose is in Gray (Gy) in radiotherapy. It is given by:

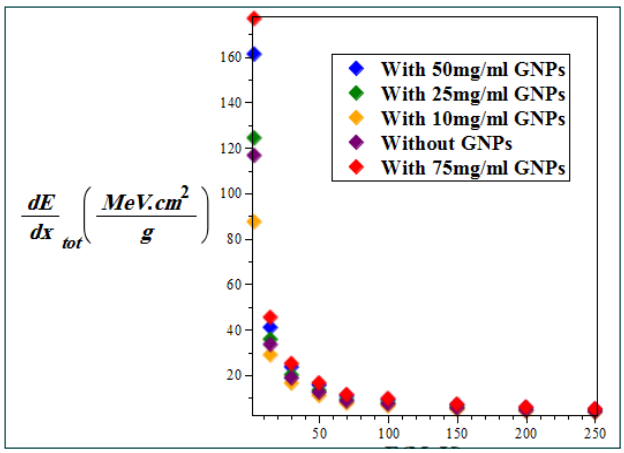

Figure.2. Comparison of total mass stopping for with/without injecting GNPs for different concentrations at BP

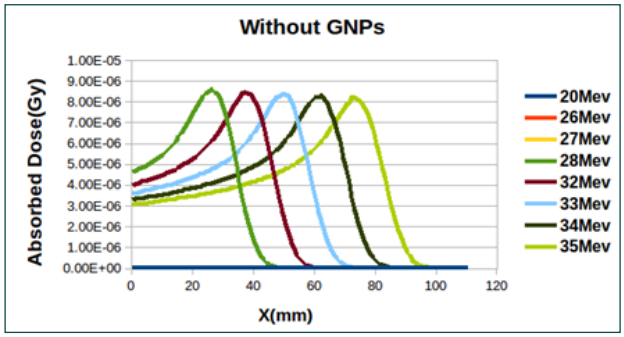

Figure.3. The absorbed dose in tumor with the size of 2 cm placed at a distance range of $4 \leq x(cm) \leq 6$ inside the breast tissue

$$D = 1.602 \times 10^{-10}.F.\frac{S}{\rho} \qquad (3)$$

where ρ is the density of the absorber material, while F is

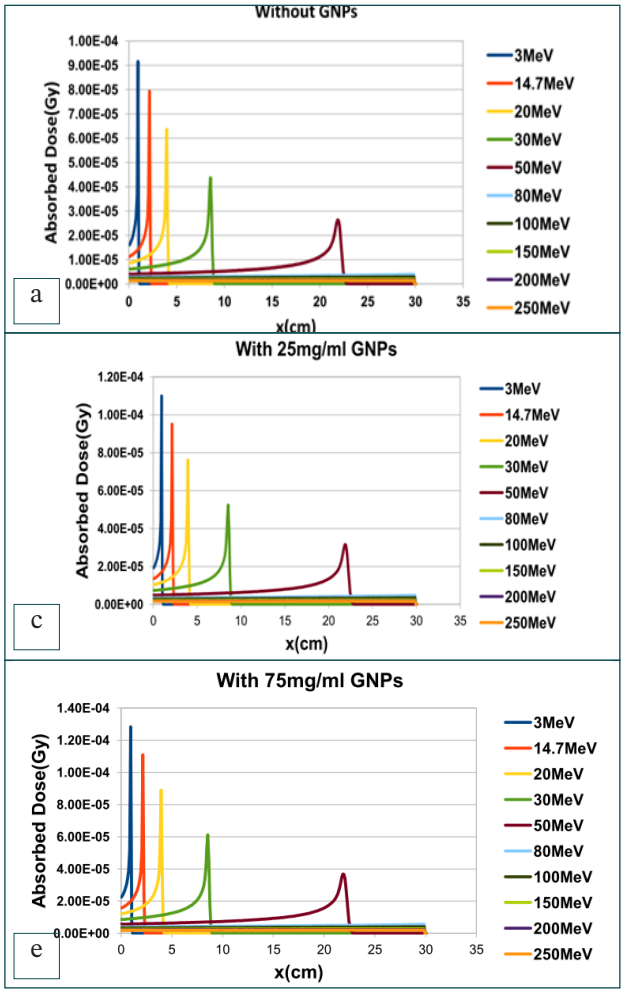

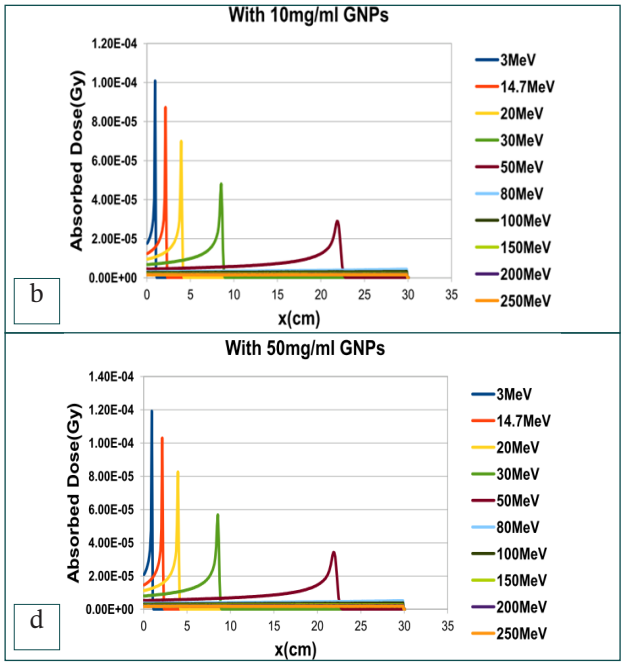

Figure.4. Comparison of the absorbed dose in the PB with and without the injection of GNPs in terms of penetration depth for different proton energies (assuming that the diameter of spherical GNPs is 50 nm)

the number of charged particles (protons) per unit (cm^2). Fig. 3 compares the absorbed dose of two cases: a) with and b) without injecting GNPs as a function of the penetration depth at different proton energies in the PB. It should be noted that at this simulation work:

$$F = 1 \times 10^6 \frac{number\ of\ particles}{cm^2}$$

Multiple Coulomb Scattering (MCS)

Protons that can pass through the material may be deflected by the atom's nucleus, and it is known as multiple Coulomb scattering (MCS). Both the protons and the nuclei are positively charged. Therefore, their interactions are mostly Columbic. Highland's formula calculates the mean scattering angle θ (12, 13):

$$\theta_0 = \frac{14.1MeV}{pv} z_p \sqrt{\frac{L}{L_R}} \left[1 + \frac{1}{9}\log_{10}\left(\frac{L}{L_R}\right)\right] rad \quad (4)$$

where p=momentum of the proton, $v = \beta c$ =proton velocity, L = target thickness, and L_R= radiation length of the target material. The radiation length is the distance from which the energy of the radiation particles decreases due to radiation losses as much as e^{-1}= (0.37) coefficient. In Fig 4, we compare the mean Coulomb scattering angle in terms of the proton energy at the range of $1 \leq E\ (MeV) \leq 250$ for injecting different concentrations of GNPs in the BP.

Range and Range straggling

We used the CSDA method to calculate the proton range. The CSDA range is obtained by integrating on the reciprocal of the total stopping power with respect to energy from E_0 to E_f, where they are initial and final energy of the proton, respectively, which is given by: (14)

$$CSDA\ R = \int_{E_f}^{E_0} \frac{dE}{S_{tot}} \quad (5)$$

In Fig. 5, the comparison of proton range variations ver-

sus proton energy at the range of $3 \leq (\mathrm{MeV}) \leq 250$ without and with the injecting of GNPs in the breast tissue is depicted as a diagram. The loss of energy of an ion in the matter is a statistical process, and it is not definite, and Bethe's equation represents only the mean energy loss. This variation was firstly obtained by Bohr, who introduced energy straggling (σ_E) :

$$\frac{d\sigma_E^2(x)}{dx} \approx \frac{1}{4\pi\epsilon_0^2} e^4 \rho_e \quad (6)$$

where ρ_e = electron density. This is valid for energy loss that is large enough for maintaining Gaussian approximation, but it is small enough when its energy can be assumed to be constant. Schulte et al. introduced the following differential equation: (15)

$$\frac{d\sigma_E^2(x)}{dx} = K(x) - 2\frac{dS(E(x))}{dx}\sigma_E^2(x) \quad (7)$$

where K (x) is represented as:

$$K(x) = z^2 \rho_e K \frac{1-\frac{1}{2}\beta^2}{1-\beta^2} \quad (8)$$

range straggling (σR), as a function of energy, is determined through the solution of the following equation:

$$\frac{d\sigma_R^2}{dx} = \frac{1}{S(E)}\frac{d\sigma_E^2(x)}{dx} \quad (9)$$

Where S (E) = the total mass stopping power. We calculated the range straggling in terms of proton energy in the breast tissue for two cases, including with and without injecting GNPs, and its diagram is shown in Fig. 6.

Amplification of radiotherapy by injecting GNPs into the tumor

In targeted cancer treatment, physicians use drugs that can better penetrate cancer cells to diagnose and treat (16,17). For this purpose, GNPs are used as a photon active element simultaneously with PB irradiation. Radiation therapy by mixing NPs increases the number of photoelectrons in the tumor due to particles with a high atomic number. As the absorption of photoelectrons into the irradiated tumor increases, the absorbed dose of the tumor enhances. Experimental studies have shown that the size of NPs and how they are distributed in different organs are related to each other. The maximum accumulation of GNPs with diameters of 20-100 and 220 nm is in the liver and spleen. Still, NPs smaller than 10 nm in diameter were observed in most organs, including the kidney, heart, lung, brain, liver, and spleen. NPs used in medicine are classified into two main groups. The first group of particles contain organic molecules as the main building material, and the second group that usually contain metals and minerals as the core (18,19), NPs (e.g. GNPs) are commonly used simultaneously with particle therapy to kill cancer cells due to their compatibility with the biological system and their low toxicity. One of the most important parameters of NPs is the choice of their synthesis method. Because the physical and chemical properties of the particles depend on it and are selected according to the type of coating agent, appropriate stabilizer, and the desired size. In order to use GNPs biologically, their surface must be functionalized, called functionalization. The functionalization of NPs is done to smarten, insensitivity of the immune system, and reduce toxicity in the body.

Depending on the application of functionalized NPs, different agents and compounds are used. For example, GNPs can be functionalized with polyethylene glycol to reduce toxicity, escape from the immune system, and as a result, have a longer durability in the bloodstream (8). Another important feature of GNPs is their easy coupling with antibodies. Therefore, GNPs are injected into the patient's body in various ways, such as intravenous injection or injection at the tumor site. In healthy tissue, endothelial cells have a regular arrangement and an impenetrable distance for NPs. Still, in tumor tissue, the arrangement of endothelial cells is irregular and has large pores, which causes high NPs of gold permeability to tumor tissue. In this process, the antibodies first guide the NPs to the target cells, and after attaching them to the target cells, they are irradiated. All cancer cells interact with the NPs and are killed by the heat generated with the collision of electromagnetic waves caused by the radiation of a particle beam with GNPs.

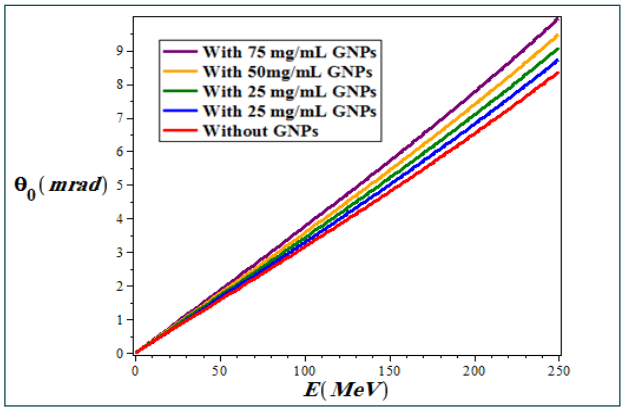

Figure.5. Comparison of the mean Coulomb scattering angle in terms of proton energy in the range of $3 \leq E\,(MeV) \leq 250$ for the injection of different concentrations of GNPs in the PB

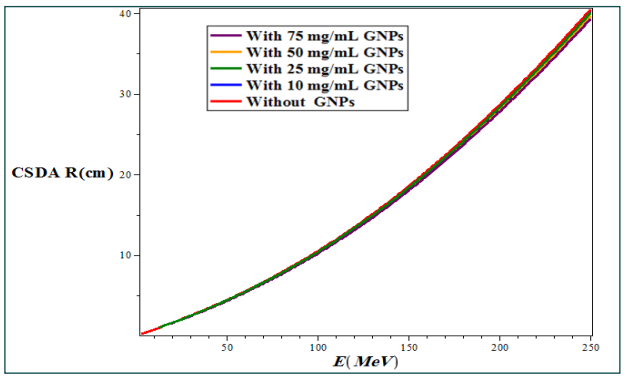

Figure.6. CSDA range variations for with/without nanoparticle injection as a function of incident proton energy

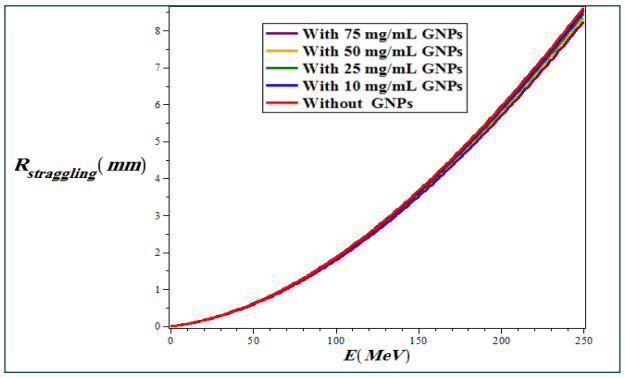

Figure.7. Comparison between variations of range straggling versus proton energy in the range of $3 \leq E\,(MeV) \leq 250$ (with/without GNPs in the breast tissue)

G7/G4MC Simulation

Recent advances in MC models have been made. However, there are still ambiguities that have not been removed. The level of agreement between the various models in predicting nuclear reaction models and laboratory data is very encouraging, but there is still enough space for improvement. The MC codes and nuclear interaction models studied in this simulation for breast cancer treatment are based on the fact that MC techniques in medical physics are rapidly increasing. This is especially true for the treatment of charged particles. MC simulation is an essential tool for designing and setting up clinical facilities that allow us to provide a detailed description of the beam line and dose delivery system. They are also widely used to design treatment rooms and protect against radiation. MC computing is a valuable tool for setting up treatment planning systems (TPS). In addition, MC codes can be a great tool for validating and possibly improving analytical TPS. In cases where experimental validity is not available or analytical methods are insufficient, MC simulation determines the dose delivered to the patient. Here, we use the G4/G7 simulation code to treat breast cancer. GATE is an advanced Open Source software and is dedicated to numerical simulations in medical imaging and radiotherapy. GATE software currently supports simulations of positron emission tomography (PET), single-photon emission computed tomography (SPECT), computed tomography (CT), and radiotherapy experiments. Using an easy-to-learn large-scale mechanism to configure highly complex experimental settings easily, GATE now plays a key role in designing the new medical imaging devices, optimizing image processing algorithms. Also, it can be used to calculate absorbed doses in radiation therapy trials. GATE is an application of GEANT4 that uses the GEANT4 library to achieve a versatile, simulated tool compatible with nuclear medicine.

RESULTS:

In Figs.2 to 7, we represented results of the total mass stopping power, absorbed dose, mean Coulomb scattering angle, CSDA range variations, and range straggling

in terms of proton energy at the range of $3 \leq E(MeV) \leq 250$ in breast tissue through G4/G7 simulation for two cases: a) with and b) without injecting gold NPs, respectively. In Fig. 8, the three-dimensional variations of the total mass stopping power and absorbed dose in terms of energy and depth of proton penetration in breast tissue are presented based on purely theoretical calculations of Bethe-Bloch's model (Eq. 2) for two cases a) with and b) without injecting GNPs using maple programming.

As shown in Fig. 2, with increasing the proton energy, the stopping power is reduced, while it is enhanced with increasing the concentration of GNPs. This is due to the density effect and also the production of secondary electrons, which means that collisions with respect to the distance between the charged particles and the atomic electrons are influenced by their atoms' interference. These atoms are polarized in the electric field of the charged particles, reducing the electron's electric field in the distance of collision, thereby reducing the stopping power. Since the relativistic effects highlight the collisions with distance, this effect can be clearly seen at the high energy levels. This effect depends on the number of polarized atoms per volume and, consequently, on the density of the materials, and therefore they are called the density effect. Typically, the ratio of the mass stopping power changes slowly in two materials with the particle energy. Also, if one of the given materials is solid and the other one is liquid or gas, this ratio will change due to the reduction in the mass stopping power of solid when the particle energy approaches the relativistic limits.

Since the tumor is placed at the penetration of 2 cm inside the breast and its width is 2 cm, the optimum energy of the Bragg peak is calculated as 32MeV (see Fig. 3). Figs. 4a, 4b, 4c, 4d, and 4e, show that by increasing the distance and energy from the beginning of the BP, the absorbed dose at the Bragg peak decreases, while the location of the Bragg peak is shifted to higher x and the lowest amount of the absorbed dose is devoted to the case of without injecting GNPs, and adding injection rate of GNPs with concentrations of 10, 25, 50, and 75 mg/ml, the percentage of the value of enhancement absorbed dose are equal to 1.1, 1.25, 1.45, and 1.75 (see the Table 1), respectively, to compared without injecting GNPs. This is because NPs with high Z, such as GNPs, increase the amount of deposited dose inside the tumor because of increasing secondary electrons. Also, our calculations show that when the protons have an energy of 250MeV, they need a phantom with a radius of more than 150 cm to put their energy into it, and only protons with the energy range of 28 to 35 MeV, deposited their energy in the selected phantom.

As shown in Fig.5, if the radiation proton energy increases, the magnitude of $\theta 0$ will increase in all states. However, the minimum $\theta 0$ in the breast tumor is related to non-injection GNPs, whereas this amount gradually increases when the injected concentration of NPs increases in the breast tumor.

As it is shown in Fig. 6, the highest CSDA range was ob-

Proton energy (MeV)	Absorbed dose (Gy)-without GNPs	Absorbed dose (Gy)-with GNPs (10ml/ml)	Absorbed dose (Gy)-with GNPs (25ml/ml)	Absorbed dose (Gy)-with GNPs (50ml/ml)	Absorbed dose (Gy)-with GNPs (50ml/ml)
3	9.02E-5	1.01E-4	1.06E-4	1. 28E-4	1.35E-4
14.7	7.98E-5	8.56E-5	9.01E-4	1.05E-4	1.17E-4
20	6.28E-5	6.63E-5	7.78E-5	8.03E-5	9.00E-5
32	4.29E-5	4.57E-5	5.21E-5	5.92E-5	6.04E-5
50	2.71E-5	2.93E-5	3.33E-5	3.64E-5	3.98E-5

Table 1. Maximum value of absorbed dose in breast-containing tumors with/without injecting GNPs for different PB energies

served when not injecting GNPs, and it slightly decreases when GNPs are increasingly injected, so that CSDA range was approached to its minimum amount at the concentration of 75 mg/ml.

As shown in Fig. 7, range straggling increases with the enhancement of proton energy for with/without GNPs. But the maximum value of this quantity is devoted to cases without GNPs injection, and the minimum amount of range straggling is related to 75 mg/ml GNPs injection. It means that with increasing the amount of GNPs injection, the straggling range reduces.

Comparisons show that there is a good agreement between total mass stopping power (Fig. 8a) associated with MC simulation under G4/G7 (Fig.2), while such correspondence can be seen between Fig. 8b and Fig. 4 (a) which is related to without-injection GNP cases.

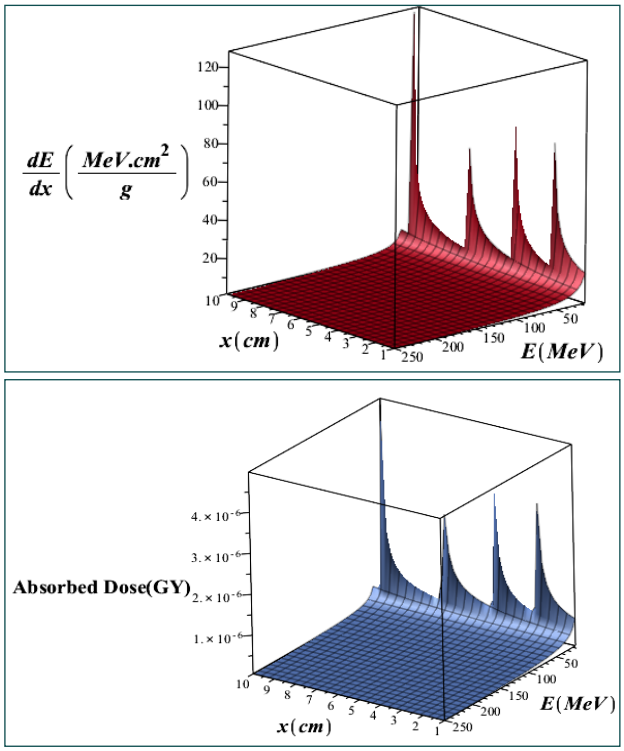

Figure.8. 3D variations of: a) mass stopping power b) absorbed dose as a function of penetration depth and proton energy in the PB without injecting GNPs regarding Bethe-Bloch theory (using Maple programming)

DISCUSSION

In this work, the G4/G7 simulation code was used in the treatment of a given tumor inside the BP. The results of our simulations show that the optimal proton energy is between 28 and 35 MeV. Also, the optimal energy of the Bragg peak is 32MeV. The represented figures show that as the proton energy increases, the penetration depth of the particle increases as well. Eventually, the number of inelastic collisions of the particle with the target material nuclei increases, which reduces the height of the Bragg peak and the transverse widening. Our simulations also show that different quantities such as total mass stopping power, adsorbed dose, mean Coulomb scattering angle, CSDA range, and range straggling depend on the concentration of injected GNPs, the type of target material, its thickness, and the proton energy. It should be noted that the percentage of increasing absorbed dose with increasing concentration of injected GNPs reaches to a maximum of 1.75%, which is due to the effect of density and increase of secondary electrons, which agreed well with the research of others (3). There is also a good agreement between the mass stopping power and the absorbed dose without injection of GNPs through the MC simulation under G4/G7 and the theoretical Bethe-Bloch's model that we performed through the Maple programming.

REFERENCES

1. Ahmad R , Royle G , Lourenço A , Schwarz M , Fracchiolla F and Ricketts K . Investigation into the effects of high-Z nano materials in proton therapy, Phys. Med. Biol. 2016; 61: 4537–4550.
2. Lacombe S, Porcel E and Scifoni E. Particle therapy and nanomedicine, state of art and research perspectives. Cancer Nano .2017: 8, 9.
3. Kuncic Z , Lacombe S. Nanoparticle radio-enhancement: principles, progress and application to cancer treatment, Phys. Med. Biol. 2018; (63) :02TR01 (27pp).
4. Kim JK, Seo SJ, Kim HT, Kim KH, Chung MH, Kim KR and Ye SJ Enhanced proton treatment in mouse tumors through proton irradiated nanoradiator effects on metallic nanoparticles Phys. Med. Biol. 57 8309 .2012.
5. Lin Y, McMahon SJ, Scarpelli M, Paganetti H and Schuemann J . Comparing gold nanoparticle enhanced radiotherapy with protons, megavoltage photons and kilovoltage photons: a MC simulation Phys. Med. Biol. 59 7675–89. 2014.
6. Lin Y, McMahon S J, Paganetti H and Schuemann J. Biological modeling of gold nanoparticle enhanced radiotherapy for proton

therapy Phys. Med. Biol. 60 4149. 2015.
7. Butterworth KT, Wyer JA, Brennan-Fournet M, Latimer CJ, Shah MB, Currell FJ and Hirst D G Variation of strand break yield for plasmid DNA irradiated with High-Z metal nanoparticles Radiat. Res. 170 381–7. 2008.
8. Porcel E, Liehn S, Remita H, Usami N, Kobayashi K, Furusawa Y, Le SC and Lacombe S .Platinum nanoparticles: a promising material for future cancer therapy? Nanotechnology 21 085103. 2010.
9. Jain S et al . Gold nanoparticle cellular uptake, toxicity and radiosensitisation in hypoxic conditions Radiother. Oncol. 110 342–7. 2014.
10. Gao J and Zheng Y MC study of secondary electron production from gold nanoparticle in PBirradiation Int. J. Cancer Ther. Oncol. 2 ,1–7. 2014.
11. Kwon J et al Dose distribution of electrons from GNPS by PBirradiation Int. J. Med. Phys. Clin. Eng. Radiat. Oncol. 4 49. 2015.
12. Wayne D Newhauser and Rui Zhang, The physics of proton therapy, Phys. Med. Biol. 60 2015;(60):R155–R209.
13. Highland VL. Some practical remarks on multiple scattering. Nuclear Instruments and Methods, vol. 129, no. 2, pp. 497499. 1975.
14. Ulmer W, Schaner B. Foundation of an analytical proton beamlet modelfor inclusion in a general proton dose calculation system. Radiation Physics andChemistry, vol. 80. 2011.
15. Schulte R et al . Conceptual design of a proton computed tomography system for applications in proton radiation therapy IEEE Trans. Nucl. Sci. 51 866–72. 2004
16. Boylestad LR , Nashelsky L. Electronic Devices and Circuit Theory: Upper Saddle River, NJ, USA: Prentice-Hall. 2012
17. Urban L. A model for multiple scattering in Geant4. Tech. Rep. 2006.
18. Salo J, Sallabi HME , Vainikainen P. Statistical Analysis of the Multiple Scattering Radio Channel. IEEE Transactions on Antennas and Propagation . Volume: 54, Issue: 11, Nov. 2006
19. Larose E , Planes T, Rossetto V, and Margerin L. Locating a small change in a multiple scattering environment Appl. Phys. Lett. 96, 204101. 2010.